16.9 Gb/s Single-Channel LWIR FSO Data Transmission with Directly Modulated QCL and MCT Detector

Mahdieh Joharifar[1], Hamza Dely[2], Laureline Durupt[3], Armands Ostrovskis[4], Richard Schatz[1], Rafael Puerta[5,1], Thomas Bonazzi[2], Gregory Maisons[3], Djamal Gacemi[2], Lu Zhang[6], Sandis Spolitis[4], Yan-Ting Sun[1], Vjačeslavs Bobrovs[4], Xianbin Yu[6], Angela Vasanelli[2], Oskars Ozolins[1,4,7], Carlo Sirtori[2] and Xiaodan Pang[1,4,7]

[1]Department of Applied Physics, KTH Royal Institute of Technology, 106 91 Stockholm, Sweden.
[2]Laboratoire de Physique de l'ENS, Département de Physique, École Normale Supérieure, Université PSL, Sorbonne Université, Université Paris Cité, CNRS, 75005 Paris, France.
[3]mirSense, 2 Bd Thomas Gobert 91120 Palaiseau, France.
[4]Institute of Telecommunications, Riga Technical University, 1048 Riga, Latvia.
[5]Ericsson Research, Ericsson AB, 164 83 Stockholm, Sweden
[6]College of Information Science and Electrical Engineering, Zhejiang University, Hangzhou 310027, China.
[7]RISE Research Institutes of Sweden, 164 40 Kista, Sweden.
mahdieh@kth.se xiaodan@kth.se

Abstract: We experimentally demonstrate a room-temperature LWIR FSO link with a 9.1-μm directly modulated QCL and an MCT detector. Net bitrate of up to 16.9 Gb/s is achieved at both 15˚C and 20˚C over a 1-meter distance. © 2024 The Author(s)

1. Introduction

The mid-wave infrared (MWIR, 3-5 μm) and the long-wave IR (LWIR, 8-12 μm) are two atmospheric transmission windows in the mid-IR region and have unique advantages for long-distance free-space optical (FSO) communications [1]. Compared with the near-IR telecom band around 1.5 μm, the MWIR and LWIR experiences significantly reduced Mie scattering from particles of a few micrometers in size, commonly found in meteorological phenomena such as dust, sand, haze, and low-altitude clouds. Moreover, their longer wavelengths ensure higher resilience against atmospheric turbulence scintillation and more relaxed eye-safety threshold [2]. Therefore, the MWIR and the LWIR can potentially offer better link availability, addressing a key limitation of FSO systems in practical applications. Several high data rate demonstrations in the MWIR window have been reported using the wavelength-conversion approach, which benefits from reusing fiber-optic components and existing multidimensional multiplexing schemes [3]-[5]. Direct emitting mid-IR sources, particularly semiconductor optoelectronic components, can facilitate smaller footprint, lower energy consumption, and higher integrability. The recent technology breakthroughs in quantum cascade laser (QCL), including room-temperature continuous-wave operation, high output power, and broad modulation bandwidth, provides a promising pathway for mid-IR FSO transceivers [6]. Several demonstrations in both MWIR and LWIR with multi-gigabit transmission rates have been reported with QCL and different types of detectors, including HgCdTe (mercury cadmium telluride, MCT) detector, quantum-well IR detectors (QWIP) and quantum cascade detector (QCD) [7]-[11]. While most existing MCT detectors typically have lower bandwidth than QWIP and QCD, they can operate in a broader spectral region covering the MWIR and LWIR simultaneously, featuring potential support for wavelength-division multiplexing (WDM).

We have previously demonstrated 8.1 Gb/s 8-level pulse amplitude modulation (PAM8) signal transmission with an LWIR QCL and a low-bandwidth MCT [12]. In this work, we employ an upgraded MCT photovoltaic detector with enhanced bandwidth to improve the system's end-to-end frequency response. We have successfully transmitted a 9 Gbaud PAM4 signal below the 6.25% overhead hard-decision forward error correction (HD-FEC) threshold of 4.5×10^{-3} [13], thanks to the enhanced characteristics of the detector. This achievement results in a net bitrate of 16.9 Gb/s, notably exceeding our prior record.

2. Experimental Setup

Figure 1(a) depicts the experimental setup. To evaluate the system performance, we employed three modulation formats, i.e., non-return-to-zero (NRZ), PAM4, and PAM6. The symbol sequences of each modulation format were obtained through the mapping of a random binary sequence containing more than one million samples, generated in MATLAB utilizing the Mersenne Twister algorithm with a shuffled seed number. To mitigate the impact of the system's bandwidth limit, we apply a root-raised-cosine (RRC) pulse shaping filter with a 0.1 roll-off factor and employ a static two-tap pre-equalization filter on the symbols. A 65 GSa/s arbitrary waveform generator (AWG) is used to convert the digital samples that are generated offline into the analog domain. The AWG output signal is combined with the DC bias current at a high-current handling bias-tee of bandwidth of 40 GHz and delivered to the QCL mount. The DM-QCL chip, operating at a central wavelength of 9.1 μm, is securely attached to a QCL mount that incorporates a Peltier thermoelectric cooler (TEC) for cooling. Figure 1(b) and (c) show the detailed digital signal processing (DSP) routines in the transmitter and receiver. Figure 1(d) shows the P-I-V curve of the QCL chip, which is measured at 15˚C. At this temperature, the laser exhibits a lasing

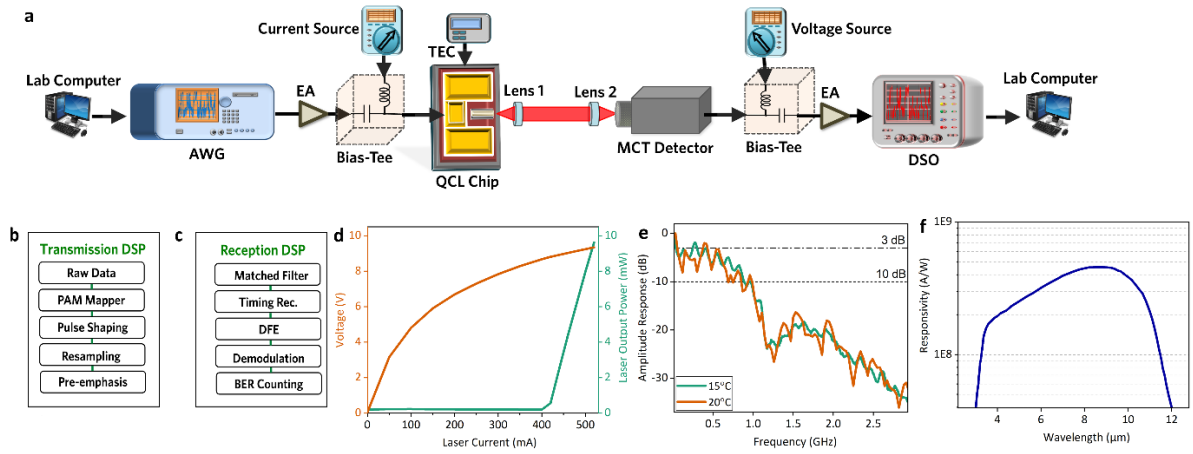

Fig. 1. (a) Experimental setup. (b),(c) Detailed DSP flow of the signal. (d) P-I-V curve of the 9.1-μm DM-QCL at 15˚C. (e). Characterized end-to-end amplitude response, including the QCL, the MCT, and all the electrical and RF components at 15˚C and 20˚C. and (f) The responsivity spectrum of the MCT detector.

threshold of approximately 400 mA, with saturation occurring at around 520 mA. The DM-QCL chip is epitaxially grown on an InP substrate using Molecular Beam Epitaxy (MBE), and the active region is comprised of a series of GaInAs wells and AlInAs barriers in strain-compensated compositions. The 4-mm single-mode distributed feedback (DFB) ridge laser is fabricated with epi-down processing and subsequently attached to a copper block.

At the receiving end, we used a commercial MCT detector (ViGO UHSM-10.6) photovoltaic detector, which operates in the 3-12 μm wavelength window at room temperature. The MCT detector is integrated with transimpedance and cooled with Peltier. Compared with our previously employed MCT detector of 750 MHz bandwidth, this detector has a Using an IR power meter at the receiver end, we calibrated the received signal power, fine-tuned it for optimization, and then swapped the power meter for the MCT detector to convert the optical signals into electrical signals. A 40 GSa/s real-time digital storage oscilloscope (DSO) converts the incoming electrical signal into digital samples to be processed offline. Figure 1 (d) exhibits the calibrated end-to-end channel amplitude response of the FSO system, which was measured at both 15 °C and 20 °C. This response covers the AWG, the DM-QCL, the MCT detector, the DSO, and all the electrical components situated in between. The end-to-end 3-dB bandwidth is measured approximately 250 MHz at 15 °C and 360 MHz at 20 °C. The 10-dB bandwidth at 15 °C is around 880 MHz, and at 20 °C is about 930 MHz. Figure 1(f) shows the MCT detector responsivity spectrum at ambient operating temperature of 20°C. The spectrum indicates that the detector has a flat broadband with a high detectivity. It can be employed in various MWIR and LWIR applications that necessitate a broad spectral range. Finally, the signal undergoes a sequence of processing steps, which include an RRC filter matched to the transmitter side, an up-sampling, timing recovery, and down-sampling procedure based on maximum variance, and a symbol-spaced decision-feedback equalizer (DFE) with 99-feedforward taps and 55-feedback taps. The bit error rate (BER) performance is then evaluated following the symbol demodulation.

3. Experimental results

We calculated the BER results to assess the FSO transmission performance with three modulation formats, including OOK, PAM4, and PAM6. We conducted consecutive sweeps of laser bias currents with constant power into the detector at two different temperature settings of 15 and 20 degrees. This sweep characterizes the trade-off between modulation depth and modulation linearity. At 15°C, we measured the BER performances of four test cases, as shown in Fig. 2 (a). For 10 Gbaud NRZ, we could achieve a BER well below the Reed–Solomon (RS) (528,514) pre-FEC limit of 2.2×10^{-5}, referred to as KR-FEC with 2.7% overhead [14]. The corresponding eye diagram is shown in the inset, where one can observe clear eye opening. This configuration results in a net bitrate of 9.7 Gb/s. The 16 Gbaud NRZ and 9 Gbaud PAM4 achieved BER below the 6.25% OH HD-FEC limit, yielding net bitrates of 15 Gb/s and 16.9 Gb/s, respectively. We also benchmark the performance with the 20%-OH soft-decision FEC (SD-FEC) limit of 2×10^{-2} [15], which has higher coding gain at the cost of higher complexity and latency yet can be relevant for long-distance ground-to-satellite LWIR FSO scenarios to prevent the need for re-transmission. In this case, the system supports up to 8 Gbaud PAM6 (20 Gb/s gross rate), corresponding to a net bitrate of 16.6 Gb/s. The eye diagram of PAM6, as shown in Fig.2(a) inset, experienced slight compression on the top and bottom edge levels, caused by the high peak-to-peak voltage swing of the driving signal to meet the stringent signal-to-noise ratio (SNR) requirement.

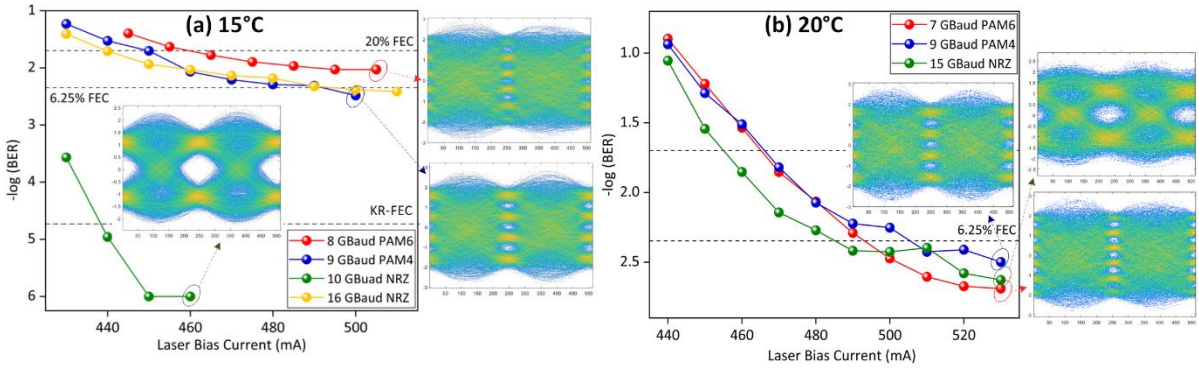

Fig. 2(a). BER results as a function of laser bias for different modulation formats at 15°C. Insets: Selected eye diagram for 8 GBaud PAM6, 9 GBaud PAM4, and 10 GBaud NRZ. (b). BER results as a function of laser bias for different modulation formats at 20°C. Insets: Selected eye diagram for 7 GBaud PAM6, 9 GBaud PAM4, and 15 GBaud NRZ.

Figure 2(b) shows the measured BER results as a function of the laser bias current at 20°C. We quantified the BER results of three configurations; 15 Gbaud NRZ, 9 Gbaud PAM4, and 7 Gbaud PAM6, all successfully reached the 6.25%-OH HD-FEC threshold, resulting in net bitrates of 14.1 Gb/s, 16.9 Gb/s and 16.4 Gb/s. Clear eye diagrams after DFE for all three test cases are observed, shown as the insets in Fig. 2(b). For both temperatures, PAM4 appears to be the optimal modulation format, considering the system tradeoff between the bandwidth and the SNR.

4. Conclusion

We implemented an LWIR FSO transmission operating at 9.1 µm with a DM-QCL and a commercial MCT detector. The system supports a net bitrate of up to 16.9 Gb/s with BER performance below the 6.25%-OH HD-FEC limit, both operating the QCL at 15°C and 20°C, significantly exceeding our previous record. We view this work as an important contribution to the realization of a comprehensive high-speed LWIR FSO network, which is envisioned to serve as a critical part of the future ICT infrastructure.

5. Acknowledgement

This work was supported in part by the EU H2020 cFLOW Project (828893), in part by the Swedish Research Council (VR) project 2019 05197 and project ‘BRAIN’ 2022 04798, in part by the COST Action CA19111 NEWFOCUS, in part by the LZP FLPP project ‘MIR FAST’ lzp-2023-1-0503, and in part by the strategic innovation program Smarter Electronic Systems - a joint venture by Vinnova, Formas and the Swedish Energy Agency A-FRONTAHUL project (2023-00659).

6. References

[1] E. Leitgeb *et al.*, "Analysis and evaluation of optimum wavelengths for free-space optical transceivers," in *Proc. ICTON* 2010, pp. 1-7.
[2] A. Delga *et al.*, "Free-space optical communications with quantum cascade lasers," in *Quantum Sensing and Nano Electronics and Photonics XVI*(2019), p. 1092617.
[3] Y. Su, et al., "150 Gbps multi-wavelength FSO transmission with 25-GHz ITU-T grid in the mid-infrared region," Optics Express **31**, 15156-15169 (2023).
[4] K. Zou, et al., "High-capacity free-space optical communications using wavelength- and mode-division-multiplexing in the mid-infrared region," Nat Commun **13**, 7662 (2022).
[5] A. E. Willner, et al., "Free-space mid-IR communications using wavelength and mode division multiplexing," Optics Communications **541**, 129518 (2023).
[6] M. Carras *et al.*, "Room-temperature continuous-wave metal grating distributed feedback quantum cascade lasers," Applied Physics Letters **96**, 161105 (2010).
[7] X. Pang *et al.*, "Gigabit free-space multi-level signal transmission with a mid-infrared quantum cascade laser operating at room temperature," Opt. Lett. **42**, 3646-3649 (2017).
[8] O. Spitz *et al.*, "Free-Space Communication With Directly Modulated Mid-Infrared Quantum Cascade Devices," IEEE Journal of Selected Topics in Quantum Electronics **28**, 1-9 (2022).
[9] P. Didier *et al.*, "Interband cascade technology for energy-efficient mid-infrared free-space communication," Photonics Research **11** (2023).
[10] H. Dely *et al.*, "10 Gbit s−1 Free Space Data Transmission at 9 µm Wavelength With Unipolar Quantum Optoelectronics," Laser & Photonics Reviews **16** (2021).
[11] X. Pang *et al.*, "11 Gb/s LWIR FSO transmission at 9.6 µm using a directly-modulated quantum cascade laser and an uncooled quantum cascade detector," in *Proc. OFC 2022*, paper Th4B.5.
[12] M. Joharifar *et al.*, "8.1 Gbps PAM8 Long-Wave IR FSO Transmission using a 9.15-µm Directly-Modulated QCL with an MCT Detector," in *Proc. OFC 2022*, paper Th1H.1.
[13] L. M. Zhang, and F. R. Kschischang, "Staircase Codes With 6% to 33% Overhead," J. Lightwave Technol. **32**, 1999-2002 (2014).
[14] "IEEE Standard for Ethernet," IEEE Std 802.3-2015 (Revision of IEEE Std 802.3-2012), 1-4017 (2016).
[15] A. Graell i Amat, and L. Schmalen, "Forward Error Correction for Optical Transponders," in *Springer Handbook of Optical Networks*, B. Mukherjee, I. Tomkos, M. Tornatore, P. Winzer, and Y. Zhao, eds. (Springer International Publishing, 2020), pp. 177-257.